RSC Advances

ROYAL SOCIETY OF CHEMISTRY

www.rsc.org/advances

A microbial fuel cell (MFC) was successfully applied for the treatment of benzene and ammonium co-contaminated groundwater.

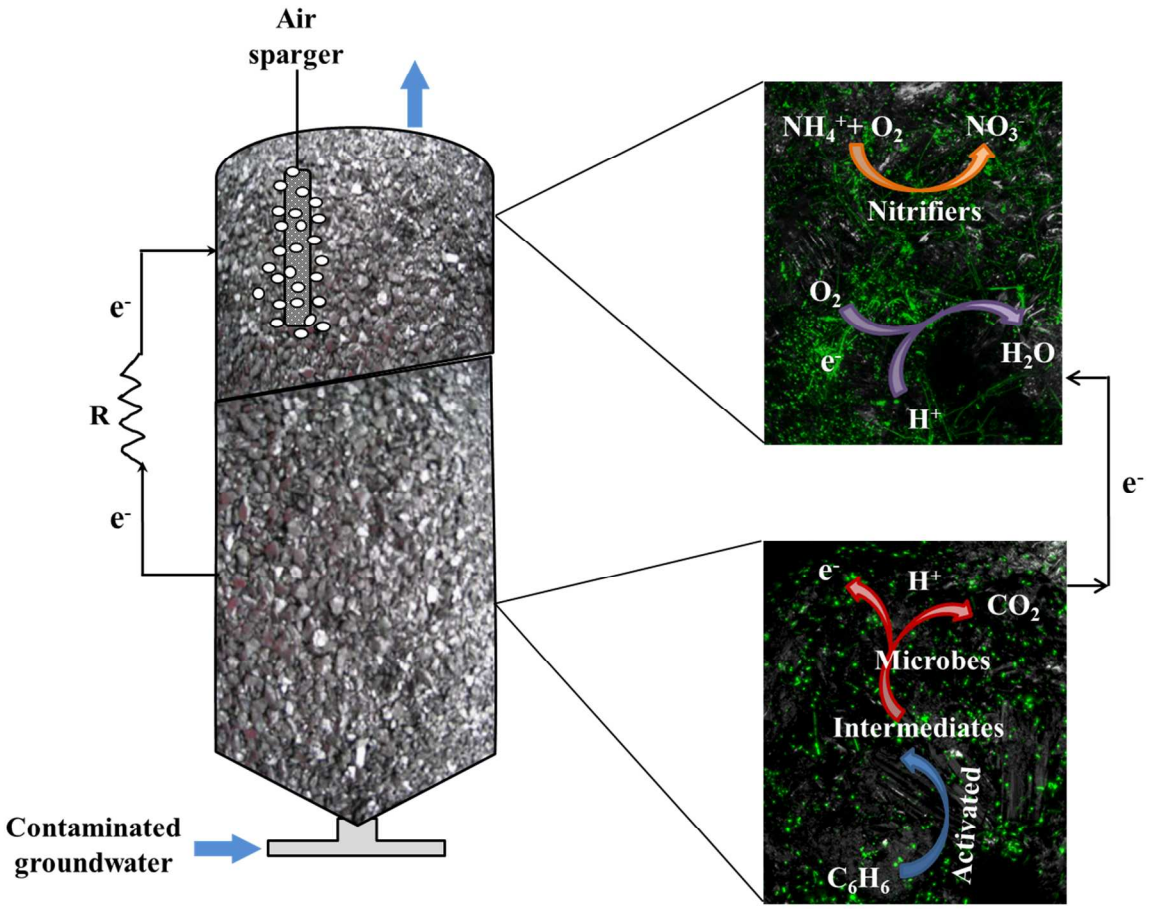

Harvesting electricity from benzene and ammonium-contaminated groundwater using a microbial fuel cell with an aerated cathode

Manman Wei,[ab] Falk Harnisch,[c] Carsten Vogt,*[a] Jörg Ahlheim,[d] Thomas R. Neu,[e] Hans H. Richnow [a]

[a] Department of Isotope Biogeochemistry, Helmholtz Centre for Environmental Research - UFZ, Permoserstraβe 15, 04318 Leipzig, Germany

[b] Faculty of Natural Cciences, Hohenheim University, 70593 Stuttgart, Germany

[c] Department of Environmental Microbiology, Helmholtz Centre for Environmental Research - UFZ, Permoserstraße 15, 04318 Leipzig, Germany

[d] Department of Groundwater Remediation, Helmholtz Centre for Environmental Research - UFZ, Permoserstraße 15, 04318 Leipzig, Germany

[e] Department of River Ecology, Helmholtz Centre for Environmental Research - UFZ, Brueckstrasse 3A, 39114, Magdeburg, Germany

* Author for correspondence:

Telephone: +49-341-235-1357; fax: +49-341-235-450822; email: carsten.vogt@ufz.de

Abstract

Groundwater contaminated with benzene and ammonium was continuously treated using a microbial fuel cell (MFC) with an aerated cathode and a control without aeration at the cathode. Benzene (~15 mg/L) was completely removed in the MFC of which 80% disappeared already at the anoxic anode. Ammonium (~20 mg/L) was oxidized to nitrate at the cathode, which was not directly linked to electricity generation. The maximum power density was 316 mW/m^3 NAC at a current density of 0.99 A/m^3 normalized by the net anodic compartment (NAC). Coulombic and energy efficiencies of 14% and 4% were obtained based on the anodic benzene degradation. The control reactor failed to generate electricity, and can be regarded as a mesocosm in which granular graphite was colonized by benzene degraders with a lower benzene removal efficiency compared to the MFC. The dominance of phylotypes affiliated to the *Chlorobiaceae*, *Rhodocyclaceae* and *Comamonadaceae* was revealed by 16S rRNA illumina sequencing in the control and the MFC anode, presumably associated with benzene degradation. Ammonium oxidation at the cathode of the MFC was mainly carried out by phylotypes belonging to the *Nitrosomonadales* and *Nitrospirales*. Compound specific isotope analysis (CSIA) indicated that benzene degradation was initially activated by monohydroxylation with molecular oxygen. The intermediates of benzene degradation pathway were subsequently oxidized accompanied by transferring electrons to the anode, leading to current production. This study provided valuable insights into the application of MFCs to treat groundwater contaminated with petroleum hydrocarbons (e.g. benzene) and ammonium.

Key words: benzene degradation; ammonium oxidation; microbial fuel cell; electricity recovery; compound-specific stable isotope analysis

1. Introduction

Remediation by microbial fuel cells (MFCs) is a promising technology for wastewater treatment due to the combination of effective pollutants removal and electricity generation.[1] Recently, the practical application of MFCs has been widely developed to treat various contaminated waters including e.g., municipal wastewater,[2] animal wastewater,[3, 4] and industrial wastewater.[5, 6] In a few cases, the effective removal of petroleum constituents from contaminated sediments or soil coupled to electricity generation have been also achieved using MFC technology.[7, 8] Many industrial activities such as oil refining and chemical industry produce wastewater containing ammonium, sulfide and petroleum hydrocarbons (e.g. BTEX, benzene, toluene, ethlylbenzene, and xylene).[9, 10] For example, the Leuna site (Saxony-Anhalt, Germany) has been a center of chemical industry for about 100 years, leading to groundwater contaminated mainly by benzene and ammonium.[11] These pollutants have been reported to cause severe environmental and public health damage.[12] A variety of remediation technologies, such as constructed wetlands,[13, 14] soil filter systems,[9] and aerated treatment ponds with biofilm promoting mats,[15] have been used to treat groundwater contaminated with benzene and ammonium from the Leuna site. However, oxygen was considered to be one of the limiting factors for efficient ammonium removal in these remediation systems.[13, 14, 16] Heterotrophic bacteria were reported to potentially compete for oxygen and inorganic nitrogen with nitrifiers, possibly resulting in

low nitrification rates under oxygen-limited conditions.[17, 18] In addition, the presence of BTEX (benzene, toluene, ethylbenzene, and xylene isomers) and their metabolic intermediates (e.g. phenol) were described to inhibit the nitrification process.[19-21] The inhibitory effect of benzene on the nitrification process, seemingly caused by the competition between benzene degraders and nitrifiers, is an obstacle to simultaneously remove benzene and ammonium using conventional treatment technologies.

It is already reported that the MFC technology has a practical potential for removing benzene at the anode. Zhang et al.[22] observed benzene degradation in contaminated marine sediments by providing a graphite electrode as an electron acceptor, demonstrating the potential of electrode-based systems for degradation of aromatic hydrocarbons in anoxic environments. Luo et al.[23] operated a packing-type MFC and found that 600 mg/L benzene was completely degraded within 24 h with simultaneous power generation when 1000 mg/L glucose was provided as the co-substrate. Simultaneous benzene biodegradation and electricity production with potassium ferricyanide as electron acceptor in a MFC was also reported by Wu et al.[24]. Due to the fast reaction kinetics, the aromatic ring of benzene was likely activated and cleaved by mono- and/or dioxygenases[12, 25] in the studies of Luo et al.[23] and Wu et al.[24], indicating aerobic or microaerobic conditions; it has been reported previously that benzene can be effectively degraded under oxygen-limited conditions.[26, 27] Nevertheless, the data indicate that benzene can be biodegraded under anoxic or oxygen-limited conditions in a MFC system, although the mentioned studies were performed under simulated and simplified conditions in the laboratory.

Ammonium removal in MFCs has been observed to occur at the cathode. He et al.[28]

reported that ammonium can be removed mainly by partial nitrification with nitrite production in a rotating-cathode MFC, although the process showed only a low coulombic efficiency (*CE*=0.34%). Subsequently, ammonium removal by simultaneous nitrification and denitrification was achieved in a MFC coupled with a nitrifying bioreactor[29] or by introducing additional oxygen into the cathode.[30-33] Notably, a denitrifying liter-scale MFC has been successfully used to enhance the total nitrogen removal in a municipal wastewater treatment facility.[34]

Therefore, MFCs are a good choice to sequentially remove benzene and ammonium due to the presence of separated anodic and cathodic compartments. Considering the complexity of contaminated groundwater, the feasibility of MFCs for contaminant removal is usually limited by high internal resistance, pH buffering, inhibition effect between co-contaminants and low efficiency of mixed culture biofilms on an electrode.[35] The practical application of a MFC for the treatment of benzene and ammonium-contaminated groundwater has not been studied yet. Hence, the objective of this study was to investigate whether a MFC can be used to remediate real groundwater contaminated with benzene and ammonium while simultaneously recovering energy. For that purpose, a MFC with an aerated cathode and a control without aeration were compared for the performance of benzene and ammonium removal as well as electricity generation. Additionally, the effect of hydraulic retention time (HRT) on the performance of the MFC was investigated. To understand the electrochemical processes occurring in the MFC, benzene and ammonium spiking as well as oxygen interruption experiments were performed in batch mode. Additionally, the degradation pathways and key players were elucidated by compound specific isotope analysis (CSIA)

and illumina sequencing.

2. Experimental

2.1. Reactor setup

Two reactors, MFC and control, were constructed as previously described by Rakoczy et al. [36] with some modifications (Fig. 1). Every reactor consisted of two cylindrical glass compartments having each a diameter of 6 cm which were separated by a Nafion-117 cation exchange membrane (CEM) (QuinTech, Göppingen, Germany). The cathode compartment (10 cm height, 330 mL total volume) was located on the top of the anode compartment (22 cm height, 680 mL total volume). Both compartments were completely filled with granular graphite of 1-6 mm diameter (Edelgraphit GmbH, Bonn, Germany) which served as electrodes. After filling with granular graphite, the anodic and cathodic compartment had a net liquid volume of 320 mL and 160 mL, respectively. A ring of stainless steel (304 SS, 2 cm length, 6 cm diameter) was used as electron collector for granular graphite at each compartment and interfaced to the external resistor. A loop between the anode and cathode compartment was added (Fig. 1), allowing the anodic effluent flowing directly into the cathodic compartment and thus eliminating proton mass transfer loss and membrane pH gradients. An air sparger linked to an air pump (EHEIM 100, Stuttgart, Germany) was installed in the cathodic compartment of the MFC to provide aeration. Continuous recirculation was generated using peristaltic pumps (Ismatec REGLO Analog MS-2/6, Wertheim, Germany) at a rate of 60 mL/min in both compartments in order to maintain well-mixed conditions. The reactors were completely covered with aluminum foil to avoid light exposure, hence inhibiting growth of phototrophic organisms.

In the control reactor, pseudo-anode and pseudo-cathode were defined as two separate compartments (corresponding to the anode and cathode compartments of the MFC), in which no electrochemical reactions occurred.

2.2. Start-up and reactor operation

Both reactors were inoculated and continuously fed with contaminated groundwater from Leuna; the composition is listed in Table 1. The groundwater was periodically taken from a nearby groundwater well and stored in a 50 L tank which was kept at 0.5 bar N_2 pressure to maintain anoxic conditions and was also connected to a cooling system to keep the temperature at 10-12 ^{o}C.

The reactors were firstly operated in continuous treatment mode (day 0-134), using 1,000 Ω external resistance and a flow rate of 0.3 mL/min, resulting in a HRT of 27 h. These parameters were only changed for polarization measurements (see 2.4.). Between day 134 and 160, the MFC was operated at the flow rates of 0.1, 0.5, 0.7, and 1.0 mL/min, corresponding to HRTs of 80, 16, 12, and 8 hours, in order to investigate the effect of varying HRTs. Once changing to a new flow rate, the MFC was running for one week to reach a stable current output before further measurements. After 160 days, benzene and ammonium spiking experiments were performed in the MFC. Briefly, 15, 30, and 50 mg/L benzene were injected into the anode which was operated in a fed-batch mode, while the cathode was running in a continuous flow mode. Subsequently, 20, 50 and 100 mg/L ammonium were injected to the cathode in a fed-batch mode, while the anode was operated in a continuous mode. Finally, through switching on or off the air pump, oxygen interruption was performed twice in the continuous flow mode in order to prove whether

oxygen was the electron acceptor.

2.3. Chemical analysis

Benzene was analyzed using a gas chromatograph equipped with a flame ionization detector (Varian CP-3800 GC, Palo Alto, CA) described elsewhere.[37] NH_4^+-N, NO_2^--N and NO_3^--N were analyzed colorimetrically as described before;[38] the detection limit was 10 μM for each compound. The pH was monitored by a pH meter (Knick, Berlin, Germany). Dissolved oxygen (DO) was measured using an optical trace sensor system (PreSens sensor spot PSt6 and FIBOX-3 minisensor oxygen meter, Regensburg, Germany) described in more detail by Balck, et al.[39] The redox potential (Eh) was measured with a pH/mV/Temp meter (Jenco Electronics 6230N, San Diego, USA). Samples for Fe^{2+} and total Fe measurements were acidified to pH 2 directly after the sampling and analyzed photometrically according to the guideline DIN 38405 D11. PO_4^{3-}, Cl^-, and SO_4^{2-} were measured using the ion chromatograph (Dionex DX500, Idstein, Germany) following the guideline EN ISO 10304-2, DIN 38405-19. Total organic carbon (TOC), inorganic carbon (IC), 5-day biological oxygen demand (BOD), and chemical oxygen demand (COD) were analyzed according to previously described methods.[15]

2.4. Electrochemical measurements and calculations

The Voltage (V) across a resistor (R) was recorded at 20 min intervals using a multimeter (Metrix MTX 3282, Paris, France). Current (I) was calculated by Ohm's law ($I = V/R$) and power (P) was calculated as $P = V \times I$. Current and power density were normalized by the net anode compartment volume (NAC). The coulombic efficiency (*CE*) was calculated as the ratio of the number of electrons recovered as charge versus the number of released electrons

by substrate removal. The energy efficiency (η) was defined as the ratio of power produced by the cell to the heat of combustion of organic substrate, and was calculated as previously described.[40] Polarization and power density curves were generated by varying the resistor from 56,000 to 100 Ω (forward). Backward polarizations were also recorded by varying resistance from 100 to 56,000 Ω; the hysteresis was comparably low (Fig. S4). The reactor was initially disconnected with the external resistance and was running under open circuit for five hours to produce a stable open circuit potential (OCP). Data for each resistor adjustment were recorded in intervals of 30 min or longer until the voltage change was less than 2 mV in 1 min. Individual anode and cathode potentials were measured using an Ag/AgCl reference electrode (Sensortechnik SE11, Meinsberg, Germany) and assumed to be +0.197 V against the standard hydrogen electrode (SHE).

2.5. Compound-specific stable isotope analysis (CSIA)

Benzene-containing influent groundwater and water from the pseudo-/anodic compartments of two reactors were extracted with pentane. The carbon and hydrogen stable isotope compositions were determined using a gas chromatograph-combustion-isotope ratio mass spectrometer system (GC-IRMS). The detailed measurement and calculation were performed as previously described.[36] The benzene degradation pathways were analyzed by comparing measured isotope composition shifts with published isotope enrichment factors (ε) in a two-dimensional isotope plot.[37, 41]

2.6. MiSeq illumina sequencing

Total DNA was extracted from graphite granules and cation exchange membranes using the FastDNA® spin Kit for soil (MP Biomedicals, Santa Ana, CA). PCR amplicons of bacterial

and archaeal 16S rRNA genes were generated using the *Bacteria*-universal primers 341F (5′-TCCTACGGGNGGCWGCAG-3′) and 785R (5′-TGACTACHVGGGTATCTAAKCC-3′) and *Archaea*-universal primers 340F (5′-TCCCTAYGGGGYGCASCAG-3′) and 915R (5′-TGTGCTCCCCCGCCAATTCCT-3′). Sequencing was performed using the illumina MiSeq platform at a commercial laboratory (LGC Genomics GmbH, Berlin, Germany). Raw data were processed using illumina CASAVA data analysis software and reads were demultiplexed according to index sequence. Overlapping regions within paired-end reads were then aligned to generate contigs. If a mismatch was discovered, the paired-end sequences involved in the assembly were discarded. OUT picking and taxonomical classification was performed at 97% identity level with Mothur 1.33. Sequence data were deposited in the Sequence Read Archive (SRA) of NCBI database under the accession number SRP044693.

2.7. Confocal Laser Scanning Microscopy (CLSM)

Biofilms attached to the granular graphite were examined with an upright confocal laser scanning microscope equipped with a super continuum light source (Leica TCS SP5X, Wetzlar, Germany). The system was controlled by the LAS AF software ver. 2.6.1. Samples were mounted in a coverwell chamber with a spacer of 2 mm. Bacteria were stained by nucleic acid specific fluorochrome SYBR Green. Settings for imaging were as followed: the line of 494 nm was used for excitation; detection was at 489-499 nm (reflection) and 505-580 nm (SYBR Green). Data sets were recorded by using the 25x NA 0.95 (overview) and 63x NA 0.9 (bacterial morphology) water immersible lenses.

2.8. Statistical analysis

Statistical analyses were performed using the SPSS 22.0 package (Chicago, IL, USA). The normality and homogeneity were assessed with a Shapiro-Wilk W test and a Levene test, respectively. Differences in benzene and ammonium removal efficiencies between the MFC and control reactor were compared with one-way AVONA tests. The Tukey′s post-hoc test was used to further evaluate the difference between the different flow rates when significant differences were found. Differences were considered to be statistically significant if $p<0.05$. The linear relationship between removed pollutant loads and power generations were further analyzed by a regression analysis.

3. Results and discussion

3.1. Overall treatment performance during continuous operation

3.1.1. Overall performance of the MFC with an aerated cathode

The MFC was continuously fed for around 130 days with contaminated groundwater containing up to 15 mg/L benzene and 20 mg/L ammonium (Table 1), generating current and achieving a constant benzene and NH_4^+-N removal (Fig. 2 and 3). During the initial stage, benzene and NH_4^+-N removal as well as current output gradually increased, probably due to the attachment and growth of ammonium- and benzene-metabolizing microorganisms from contaminated groundwater. After approximately two months, benzene and NH_4^+-N removal became relatively stable, indicating that electrochemical active biofilms had been fully developed, reflected also by a stable current generation (Fig. 3). In the anodic effluent of the MFC, roughly 80% of benzene was removed whereas NH_4^+-N concentrations decreased only slightly (~5%). The remaining benzene (20%) was removed at the cathode, resulting in an

overall benzene removal efficiency of 100% in the cathodic effluent. Ammonium disappeared completely in the cathodic effluent, showing finally 100% removal efficiency. In summary, benzene was removed mainly (80%) in the anodic compartment and NH_4^+-N was removed solely in the cathodic compartment of the MFC. Sequential removal of benzene and ammonium in the different compartments avoided putative negative effects of benzene and benzene degraders on the nitrification process which have been previously reported.[15, 16] During steady stage, the MFC generated current between 200 and 250 μA and a current density of 0.6~0.8 A/m^3 NAC was obtained (Fig. 3) when being operated at 1,000 Ω.

Comparing the results of this study with data for benzene and ammonium removal from other remediation technologies, similar benzene removal rates but higher ammonium removal rates were achieved in our MFC system, even only considering their best removal efficiencies achieved during summer. For example, Seeger et al.[13] reported 81%-99% benzene removal and 40-50% NH_4^+-N removal in a planted constructed wetland. A novel aerated treatment pond exhibited approximately 100% benzene concentration reduction, whereas ammonium concentrations decreased only slightly from around 59 mg/L at the inflow to 56 mg/L in the outflow, indicating no significant NH_4^+-N removal during continuous operation.[15] Recently, Rakoczy et al.[36] investigated the treatment of benzene and sulfide-contaminated groundwater using a MFC over a period of 770 days and obtained a maximum current output of approximately 250 μA in a continuous flow mode, which is comparable to the outcome of our study.

3.1.2. Overall performance of the control reactor without aeration

In the control reactor, benzene removal in both pseudo-anodic and cathodic effluent gradually

increased during the initial microbial enrichment, and then achieved steady removal efficiencies of 60% and 80%, respectively (Fig. 2). Compared to the MFC, less benzene (20% lower) was removed in the control reactor ($p<0.05$), indicating enhanced benzene degradation in the anode compartment of the MFC. Ammonium was only slightly removed (<10%) in the control, similar to the anode of the MFC. A low noise current (< 5 μA) was observed in the control, hence current was not efficiently generated (Fig. S2). In MFCs, the electrochemical potential difference of anode and cathode, depending on the redox potential of the electron donor and the terminal electron acceptor, determines the possibility and extent of generated current.[42] As nearly the same anode and cathode potentials were observed in the control (data not shown), no electromotive force was obtained and thus no current generated. Therefore, the control reactor without aeration can be regarded as a benzene-degrading mesocosm in which granular graphite was colonized by benzene degraders but not served as electron donor or acceptor.

3.2. Mechanisms of benzene and ammonium removal

3.2.1. Benzene removal mechanism

CSIA was performed in order to identify the initial activation mechanisms of benzene degradation in the MFC and the control reactor. The initial attack on thermodynamically very stable benzene is critical for its degradation process. Combined carbon and hydrogen isotope fractionation has been proved to be a powerful tool for the characterization of initial metabolic reactions for benzene biodegradation.[37, 41] Carbon and hydrogen isotope fractionations of benzene were significantly higher in the control compared to the MFC (Fig. S3). However, two dimensional plots of carbon versus hydrogen isotope fractionation were

similar for both MFC and control (Fig. 4), indicating that isotope fractionation was masked in the MFC. The detected values matched with those indicative for benzene monooxygenation to phenol catalyzed by a monooxygenase (Fig. 4). The produced phenol might be further transformed into catechol by a second monooxygenation and also the other possible intermediates after a possible *ortho* or *meta* ring cleavage of catechol.[43, 44] Monohydroxylation as benzene activation step was also identified in the anodic reaction of a MFC for treating benzene and sulfide-contaminated groundwater.[36] However, we cannot exclude that benzene was actually anaerobically activated and degraded by a mechanism producing similar carbon and hydrogen isotope fractionation as observed for aerobic monohydroxylation, as different anaerobic benzene activation mechanisms are currently proposed: an anaerobic hydroxylation to phenol[45] or a carboxylation to benzoate.[46, 47] In any case, the intermediates of the initial benzene activation steps were probably further oxidized anaerobically and accelerate electricity generation by transferring the released electrons to the anode. This is also supported by our electrochemical results (see 3.4.) and the fact besides benzene, no other electron donors were provided by the contaminated groundwater.

3.2.2. Ammonium removal mechanism

At the cathode of the MFC, ammonium was mainly oxidized to nitrate by nitrification, as indicated by an increase of NO_3^--N (Fig. S1). In the control and the anode of the MFC, nitrite and nitrate concentrations were extremely low (data not shown), showing that ammonium removal by nitrification activity was negligible; the oxygen concentrations were obviously too low for nitrification, as previously observed in an aerated treatment pond with biofilm promoting mats at the Leuna field site.[16] The small ammonium losses in the control reactor

and the anode compartment of the MFC might be due to physical-chemical processes, e.g. adsorption or volatilization.[4, 48]

3.3. Effect of the flow rate on the performance of the MFC

To determine the effect of HRTs, different flow rates were used to study benzene and NH_4^+-N removal performance as well as power generation in the MFC. As shown in Fig. 5A, benzene removal at the anode decreased from 80% at a flow rate of 0.3 mL/min (27 h HRT) to 40% at a flow rate of 1.0 mL/min (8 h HRT). At a flow rate of 0.1 mL/min (80 h HRT), benzene was completely removed already at the anode. However, 100% benzene removal efficiency was always obtained in the final cathodic effluent at the five studied HRTs. At the lower flow rate (0.1 and 0.3 mL/min), ammonium was completely removed (Fig. 5A). At flow rates higher than 0.3 mL/min, the removal efficiencies decreased gradually to around 70% at a flow rate of 1.0 mL/min, implying that nitrification was limited at the shorter HRT.

The maximum power density of 316 mW/m^3 NAC was achieved at a current of 0.99 A/m^3, when the MFC was operated at the flow rate of 0.3 mL/min (Fig. 5B). As shown by the polarization and power density curves, lower performances were obtained at higher or lower flow rates. The electrode potentials as a function of current density were also examined at different flow rates (Fig. 5C). As expected from the removal data, it was observed that the cathodic potentials were not affected by the different flow rates. The anodic OCP values shown at zero current density were also similar under the different flow rates, demonstrating an excellent stability of the system. The electrode polarization showed very different profiles for the anodic potentials at the different flow rates. Therefore, the difference of power density at the different flow rates was a result of the polarization behavior of the anodic potentials,

indicating that anodic benzene oxidation was rate-limiting and thus determined electricity generation. In order to confirm this finding, subsequent benzene injection experiments were performed and also approved that benzene served as the main anodic electron donor in the MFC (Fig. 6A).

Coulombic efficiencies of 28 ± 4.7%, 14 ± 3.4%, 10 ± 1.2%, 8 ± 1.4% and 7 ± 0.9% were obtained at the increased flow rates of 0.1, 0.3, 0.5, 0.7, and 1.0 mL/min, respectively; analogously, energy efficiencies of 8 ± 1.3%, 4 ± 0.9%, 3 ± 0.3%, 2 ± 0.3% and 1.2 ± 0.2% were achieved. The lower coulombic and energy efficiencies at higher flow rates are indicative for incomplete benzene degradation, eventually resulting in a lower number of electrons transferred to the anode. The data also indicate that a substantial number of electrons were generally not transported to the anode, probably caused by the use of penetrating oxygen or alternative substances as electron acceptors (e.g. carbonate leading to methanogenesis or organic or inorganic metabolites upon fermentation processes). Notably, the MFC with aerated cathode was more efficient with regard to benzene degradation than the ferricyanide-based MFC described recently by Wu et al.[24], which produced a power density of 2.1 mW/m^2 and showed a coulombic efficiency of 3.3%, at slightly lower benzene loadings and slightly higher benzene degradation rates. In subsequent experiment, a flow rate of 0.3 mL/min was used due to the maximum power density and high pollutant removal performance achieved at this date.

3.4. Detection of electrochemical reaction in the MFC

Although the complete degradation of benzene can theoretically release 30 electrons,[24] current generation strongly depends on whether electrons from benzene oxidation can be

efficiently transferred to the anode. In our study, when 15 mg/L benzene was injected into the anode, the current rapidly increased from around 240 to 350 μA within 3 h; subsequently, the current gradually decreased corresponding to decreasing benzene concentrations (Fig. 6A). Injecting higher benzene concentrations of 30 and 50 mg/L generated higher current maxima of 415 and 450 μA, respectively. A linear correlation was obtained between the current and the concentration of benzene at the anode (Fig. 6D), demonstrating that benzene oxidation was the main anodic reaction, and that the released electrons were efficiently delivered to the anode. In contrast, increasing ammonium concentrations by injection of 20, 50, 100 mg/L NH_4^+-N did not affect the current output (Fig. 6B), indicating that cathodic ammonium oxidation did not limit electricity generation. Subsequently, the effects of varying oxygen concentrations at the cathode were investigated (Fig. 6C). When the supply of oxygen at the cathode was stopped, the DO concentration gradually decreased from about 6 to 1 mg/L, and the current also decreased from about 300 to 60 μA. The current generation immediately increased when oxygen was again supplied and the DO concentration increased. Hence, the DO concentration was coupled to current generation, suggesting that oxygen was the main terminal electron acceptor at the cathode.

As NH_4^+-N can release maximally eight electrons via oxidation to nitrate, ammonium can theoretically serve as an anodic electron donor.[28] However, ammonium as a direct anodic fuel for electricity generation has not been demonstrated experimentally yet. In our study, ammonium was completely oxidized to nitrate at the cathode by nitrifying microorganisms (Fig. S1). Our results demonstrate that the released electrons were not involved in electrochemical reactions; probably, the electrons were directly taken by nitrifiers, explaining

why ammonium consumption was not directly connected to electricity generation in the MFC. You et al.[49] showed that additional protons produced from ammonium oxidation can reduce the ohmic resistance and maintain the pH balance in the absence of a phosphate buffer, which can contribute to the electricity generation process. Recently, it was also reported that the oxygen reduction relied on the nitrification activity at the biocathode, at least to some extent.[50] In this study, the contaminated groundwater from the Leuna site probably had a good buffer capacity, so that biological nitrification was not directly linked with current generation.

Based on these results, the anodic and cathodic reactions occurred in the MFC are described by the following equations, with the assumption of complete oxidation of benzene.

Anode: $C_6H_6 + 12\ H_2O \rightarrow 6\ CO_2 + 30e^- + 10H^+$ (1)

Cathode: $O_2 + 4\ H^+ + 4e^- \rightarrow 2\ H_2O$ (2)

Overall reaction: $C_6H_6 + 7.5\ O_2 \rightarrow 6\ CO_2 + 3\ H_2O$ (3)

Coulombic and energy efficiencies at the different flow rate were calculated according to the electrochemical reactions shown in equations 1-3.

3.5. Analysis of microbial communities in the MFC and the control

3.5.1 Bacterial community analysis

Confocal laser scanning microscopy images demonstrated that significant biofilms were formed around the granular graphite in both MFC and control (Fig. S5). The compositions of bacterial communities colonizing the pseudo-/anode, CEM and pseudo-/cathode are shown in Figure 7A. The anode of the MFC and the control reactor were mainly colonized by bacterial phylotypes belonging to the *Chlorobiales*, *Rhodocyclales*, and *Burkholderiales*. The family

Chlorobiaceae in the *Chlorobiales* accounted for ~15% and 41% of the pseudo-/anodic bacterial communities in the control and MFC, respectively. Although *Chlorobiales* are known as anaerobic photoautotrophs, several recent studies suggest that they are able to perform anaerobic dark respiration by the breakdown of organic substrates when sulfide is not used as electron donor.[51, 52] *Chlorobiales* were also identified as the dominant phylotypes in benzene degrading enrichment cultures under nitrate-reducing conditions[41, 53] indicating that *Chlorobiales* can participate in degradation of benzene or its intermediate metabolites. Large percentages of *Rhodocyclaceae* of 43% and 21% (belonging to *Rhodocyclales*) were observed at the pseudo-/anode of the control and MFC respectively, indicating as well a role of these phylotypes upon benzene degradation; correspondingly, phylotypes of this family were shown to be associated with anaerobic benzene degradation either by DNA-stable isotope probing with ^{13}C-labelled benzene[53, 54] or by phylogenetic analysis of benzene-degrading enrichment cultures.[55] The *Comamonadaceae* within the order of *Burkholderiales*, accounting for 5% and 6% of bacterial communities at the pseudo-/anode of the control and MFC, were also shown to be involved in benzene degradation.[53, 56] Overall, the dominance of these potential benzene degraders implies that those were actually related to benzene degradation in both MFC and control. The whole control reactor, including pseudo-anode, CEM and pseudo-cathode, were colonized by similar bacteria with slightly different abundances, again supporting the view that it is a homogenous mesocosm.

Different from the bacterial community at the anode, the dominant bacteria orders at the cathode of the MFC were *Nitrospirales* (18%), *Burkholderiales* (15%), *Rhodocyclales* (7%), *Nitrosomonadales* (4.5%), and *Rhizobiales* (4%). Obviously, the dominant families of

Comamonadaceae and *Rhodocyclaceae* affiliated to *Burkholderiales* and *Rhodocyclales* were able to degrade the residual benzene from the anode.[53] Phylotypes affiliated to *Nitrosomonadales* and *Nitrospirales* belong to the genera of *Nitrosovibrio* and *Nitrospira*, which presented the dominant ammonia-oxidizing and nitrite-oxidizing bacteria respectively.[57, 58] They were also identified as dominant nitrifying bacteria in wastewater treatment plants and MFC systems for nitrogen removal.[31, 59] The data suggests that ammonium was firstly oxidized to nitrite by *Nitrosovibrio*, then nitrite was further oxidized to nitrate by *Nitrospira*, leading to a high rate of nitrification at the cathode of the MFC.

3.5.2 Archaeal community analysis

The compositions of archaeal communities were shown in Fig. 7B. The archaeal communities were dominated by phylotypes belonging to the acetoclastic *Methanosarcinales* (64-76%), and hydrogenotrophic *Methanomicrobiales* (1.5-8%) in the three parts of control and the anode of the MFC (Fig. 7B). Methanogens can compete for substrates with electrochemically active microorganisms and hence reduce electron recovery.[60] It was however shown that electrochemically active microorganisms can outcompete acetoclastic methanogens for organic substrates in MFCs, eliminating electron consumption by methanogens.[60, 61] As the acetoclastic *Methanosarcinales* were the predominant archaea at the MFC anode, electron loss by methanogenesis was probably rather minor. Notably, *Methanosarcinales* and *Methanomicrobiales* have been also identified as syntrophic methanogens in anaerobic benzene-degrading enrichment cultures.[62, 63]

Different from the archaeal communities in the control and the anode of the MFC, the CEM and cathode of the MFC was dominated by unclassified *Euyarchaeota* (46%), unclassified

archaea (39%) and *Methanosarcinales* (12%). Possibly, archaea from anoxic groundwater were not able to grow at the aerobic cathode of the MFC due to the completely different physicochemical conditions.

Due to the complexity of the anode biofilm, it was very difficult to elucidate concrete electrochemical mechanisms at the anode, e.g. identifying the microorganisms actually transferring electrons to the anode. However, various dominant bacterial phylotypes were identified in the MFC, suggesting that the electrons were transferred to the anode after the initial activation reaction by monohydroxylation rather by a network of microorganisms, using different metabolites of benzene degradation as substrates, than by a single organism. These processes might be syntrophic; such syntrophic processes have been described to govern anaerobic benzene degradation in both benzene-degrading enrichment cultures and in situ benzene-degrading columns.[63]

4. Conclusions

This study demonstrated the principal feasibility of treating benzene and ammonium contaminated groundwater by a MFC equipped with an aerated cathode. Benzene was initially activated by enzymatic monohydroxylation at the oxygen-limited anode; the further anaerobic oxidation of the intermediate metabolites released electrons, which were transferred to the anode and eventually captured by oxygen, driving oxygen reduction and accelerating electricity production. Nitrification took place at the aerated cathode of the MFC and was catalyzed by nitrifiers; the process was not directly linked to electricity generation. Although it is promising that nitrification occurred in high rate at the cathode of the MFC, the accumulated nitrate still needs to be removed by an additional treatment reactor. Further

research is of particular interest in order i) to promote simultaneous benzene and ammonium removal using an anoxic cathode MFC, e.g. by addition of nitrite to accelerate anaerobic ammonium oxidation, avoiding the need of aeration, or the set-up of an additional denitrification reactor, or ii) to develop and test a scaling-up application under field conditions.

Acknowledgement

This work was financially supported by the Helmholtz Centre for Environmental Research-UFZ in the scope of the SAFIRA II Research Project (Revitalization of Contaminated Land and Groundwater at Megasites, subproject "Compartment Transfer-CoTra") and within the Research Programme "Terrestrial Environment".

Falk Harnisch acknowledges the support by the BMBF (Research Award "Next generation biotechnological processes - Biotechnology 2020+") and the Helmholtz-Association (Young Investigators Group).

References

1. B. E. Logan and J. M. Regan, *Environ. Sci. Technol.*, 2006, **40**, 5172-5180.
2. Y. Feng, W. He, J. Liu, X. Wang, Y. Qu and N. Ren, *Bioresour. Technol.*, 2014, **156**, 132-138.
3. L. Zhuang, Y. Zheng, S. Zhou, Y. Yuan, H. Yuan and Y. Chen, *Bioresour. Technol.*, 2012, **106**, 82-88.
4. J. R. Kim, Y. Zuo, J. M. Regan and B. E. Logan, *Biotechnol. Bioeng.*, 2008, **99**, 1120-1127.

5. B. Cercado-Quezada, M. L. Delia and A. Bergel, *Bioresour. Technol.*, 2010, **101**, 2748-2754.

6. P. T. Ha, T. K. Lee, B. E. Rittmann, J. Park and I. S. Chang, *Environ. Sci. Technol.*, 2012, **46**, 3022-3030.

7. J. M. Morris and S. Jin, *J. Hazard. Mater.*, 2012, **213-214**, 474-477.

8. X. Wang, Z. Cai, Q. Zhou, Z. Zhang and C. Chen, *Biotechnol. Bioeng.*, 2012, **109**, 426-433.

9. M. Afferden, K. Z. Rahman, P. Mosig, C. De Biase, M. Thullner, S. E. Oswald and R. A. Muller, *Water Res.*, 2011, **45**, 5063-5074.

10. A. Olmos, P. Olguin, C. Fajardo, E. Razo and O. Monroy, *Energy & Fuels*, 2004, **18**, 302-304.

11. M. Voyevoda, W. Geyer, P. Mosig, E. M. Seeger and S. Mothes, *CLEAN - Soil, Air, Water*, 2012, **40**, 817-822.

12. D. T. Gibson, *Science*, 1968, **161**, 1093-1097.

13. E. M. Seeger, P. Kuschk, H. Fazekas, P. Grathwohl and M. Kaestner, *Environ. Pollut.*, 2011, **159**, 3769-3776.

14. E. M. Seeger, U. Maier, P. Grathwohl, P. Kuschk and M. Kaestner, *Water Res.*, 2013, **47**, 769-780.

15. S. Jechalke, C. Vogt, N. Reiche, A. G. Franchini, H. Borsdorf, T. R. Neu and H. H. Richnow, *Water Res.*, 2010, **44**, 1785-1796.

16. S. Jechalke, M. Rosell, C. Vogt and H. H. Richnow, *Water Environ. Res.*, 2011, **83**, 622-626.

17. B. Ma, Y. Peng, S. Zhang, J. Wang, Y. Gan, J. Chang, S. Wang, S. Wang and G. Zhu, *Bioresour. Technol.*, 2013, **129**, 606-611.

18. J. Truu, K. Nurk, J. Juhanson and U. Mander, *J. Environ. Sci. Heal. A*, 2005, **40**, 1191-1200.

19. C. Ben-Youssef, A. Zepeda, A.-C. Texier and J. Gomez, *Chem. Eng. J.*, 2009, **152**, 264-270.

20. E. G. Lauchnor, T. S. Radniecki and L. Semprini, *Biotechnol. Bioeng.*, 2011, **108**, 750-757.

21. T. S. Radniecki, M. E. Dolan and L. Semprini, *Environ. Sci. Technol.*, 2008, **42**, 4093-4098.

22. T. Zhang, S. M. Gannon, K. P. Nevin, A. E. Franks and D. R. Lovley, *Environ. Microbiol.*, 2010, **12**, 1011-1120.

23. H. Luo, C. Zhang, H. Song, G. Liu and R. Zhang, *Acta Sci. Nat. Univ. Sunyatseni*, 2010, **49**, 113-118.

24. C. H. Wu, C. Y. Lai, C. W. Lin and M. H. Kao, *CLEAN - Soil, Air, Water*, 2013, **41**, 390-395.

25. F. H. Vaillancourt, J. T. Bolin and L. D. Eltis, *Crit. Rev. Biochem. Mol. Biol.* , 2006, **41**, 241-267.

26. A. Fahy, T. J. McGenity, K. N. Timmis and A. S. Ball, *FEMS Microbiol. Ecol.*, 2006, **58**, 260-270.

27. L. Yerushalmi, J. F. Lascourreges and S. R. Guiot, *Biotechnol. Bioeng.*, 2002, **79**, 347-355.

28. Z. He, J. Kan, Y. Wang, Y. Huang, F. Mansfeld and K. H. Nealson, *Environ. Sci. Technol.*, 2009, **43**, 3391-3397.

29. B. Virdis, K. Rabaey, Z. Yuan and J. Keller, *Water Res.*, 2008, **42**, 3013-3024.

30. B. Virdis, K. Rabaey, R. A. Rozendal, Z. Yuan and J. Keller, *Water Res.*, 2010, **44**, 2970-2980.

31. C. P. Yu, Z. Liang, A. Das and Z. Hu, *Water Res.*, 2011, **45**, 1157-1164.

32. H. Yan, T. Saito and J. M. Regan, *Water Res.*, 2012, **46**, 2215-2224.

33. F. Zhang and Z. He, *J. Chem. Tech. Biotech.*, 2012, **87**, 153-159.

34. F. Zhang, Z. Ge, J. Grimaud, J. Hurst and Z. He, *Environ. Sci. Technol.*, 2013, **47**, 4941-4948.

35. R. A. Rozendal, H. V. Hamelers, K. Rabaey, J. Keller and C. J. Buisman, *Trends Biotechnol.*, 2008, **26**, 450-459.

36. J. Rakoczy, S. Feisthauer, K. Wasmund, P. Bombach, T. R. Neu, C. Vogt and H. H. Richnow, *Biotechnol. Bioeng.*, 2013, **110**, 3104-3113.

37. A. Fischer, I. Herklotz, S. Herrmann, M. Thullner, S. A. Weelink, A. J. Stams, M. Schlomann, H. H. Richnow and C. Vogt, *Environ. Sci. Technol.*, 2008, **42**, 4356-4363.

38. A. Bollmann, E. French and J. L. Laanbroek, in *Methods in enzymology*, eds. J. Abelson, I. S. Melvin, S. P. Colowick and A. K. Nathan, Elsevier, Oxford, USA, Editon edn., 2011, vol. Research on nitrification and related processes, part A, pp. 55-88.

39. G. U. Balcke, S. Wegener, B. Kiesel, D. Benndorf, M. Schlomann and C. Vogt,

Biodegradation, 2008, **19**, 507-518.

40. B. E. Logan, B. Hamelers, R. Rozendal, U. Schroder, R. G. Keller, S. Freguia, P. Aelterman, W. Verstraete and K. Rabaey, *Environ. Sci. Technol.*, 2006, **40**, 5181-5191.

41. S. A. Mancini, C. E. Devine, M. Elsner, M. E. Nandi, A. C. Ulrich, E. A. Edwards and B. S. Lollar, *Environ. Sci. Technol.*, 2008, **42**, 8290-8296.

42. K. C. Wrighton and J. D. Coates, *Microbe.*, 2009, **4**, 281-287.

43. L. Yerushalmi, J. F. Lascourreges, C. Rhofir and S. R. Guiot, *Biodegradation*, 2001, **12**, 379-391.

44. S. Zaki, *J. Appl. Sci. Environ. Mgt. September*, 2006, **10**, 75-81.

45. T. Zhang, P. L. Tremblay, A. K. Chaurasia, J. A. Smith, T. S. Bain and D. R. Lovley, *Appl. Environ. Microbiol.*, 2013, **79**, 7800-7806.

46. N. Abu Laban, D. Selesi, T. Rattei, P. Tischler and R. U. Meckenstock, *Environ. Microbiol.*, 2010, **12**, 2783-2796.

47. F. Luo, R. Gitiafroz, C. E. Devine, Y. Gong, L. A. Hug, L. Raskin and E. A. Edwards, *Appl. Environ. Microbiol.*, 2014, **80**, 4095-4107.

48. H. Yan and J. M. Regen, *Biotechnol. Bioeng.*, 2013, **110**, 785-791.

49. S. J. You, N. Q. Ren, Q. L. Zhao, P. D. Kiely, J. Y. Wang, F. L. Yang, L. Fu and L. Peng, *Biosens. Bioelectron.*, 2009, **24**, 3698-3701.

50. Y. Du, Y. J. Feng, Y. Dong, Y. P. Qu, J. Liu, X. T. Zhou and N. Q. Ren, *Rsc Advances*, 2014, **4**, 34350-34355.

51. X. Feng, K. H. Tang, R. E. Blankenship and Y. J. Tang, *J. Biol. Chem.*, 2010, **285**,

39544-39550.

52. J. P. Badalamenti, C. I. Torres and R. Krajmalnik-Brown, *Biotechnol. Bioeng.*, 2013, **14**, 1020-1027.

53. B. M. van der Zaan, F. T. Saia, A. J. Stams, C. M. Plugge, W. M. de Vos, H. Smidt, A. A. Langenhoff and J. Gerritse, *Environ. Microbiol.*, 2012, **14**, 1171-1181.

54. J. S. Liou, C. M. Derito and E. L. Madsen, *Environ. Microbiol.*, 2008, **10**, 1964-1977.

55. Y. Kasai, Y. Takahata, M. Manefield and K. Watanabe, *Appl. Environ. Microbiol.*, 2006, **72**, 3586-3592.

56. D. Perez-Pantoja, R. Donoso, L. Agullo, M. Cordova, M. Seeger, D. H. Pieper and B. Gonzalez, *Environ. Microbiol.*, 2012, **14**, 1091-1117.

57. M. Meincke, E. Krieg and E. Bock, *Appl. Environ. Microbiol.*, 1989, **55**, 2108-2110.

58. S. Lucker, M. Wagner, F. Maixner, E. Pelletier, H. Koch, B. Vacherie, T. Rattei, J. S. S. Damste, E. Spieck, D. Le Paslier and H. Daims, *PNAS*, 2010, **107**, 13479-13484.

59. Y. T. Tu, P. C. Chiang, J. Yang, S. H. Chen and C. M. Kao, *J. Hydrol.*, 2014, **510**, 70-78.

60. S. Jung and J. M. Regan, *Appl. Environ. Microbiol.*, 2011, **77**, 564-571.

61. H. S. Lee, P. Prathap, K. M. Andrew, I. T. Ce´sar and B. E. Rittmann, *Water Res.*, 2008, **42**, 1501-1510.

62. N. Sakai, F. Kurisu, O. Yagi, F. Nakajima and K. Yamamoto, *J. Biosci. Bioeng.*, 2009, **108**, 501-507.

591 63. S. Herrmann, S. Kleinsteuber, A. Chatzinotas, S. Kuppardt, T. Lueders, H. H.
592 Richnow and C. Vogt, *Environ. Microbiol.*, 2010, **12**, 401-411.

593

Figure and table legends

Table 1: Physico-chemical properties of contaminated groundwater used in this study

Figure 1: Schematic view (A) and picture (B) of the MFC and the control used in this study.

Figure 2: Benzene and NH_4^+-N removal in the MFC (A) and the control (B) during continuous treatment of contaminated groundwater.
*represents significant higher removal efficiency ($p<0.05$) in the MFC compared to the control at the same sampling time.

Figure 3: Current generation in the MFC during continuous treatment of contaminated groundwater.

Figure 4: Two-dimensional isotope plot of $\Delta\delta^{13}C$ versus $\Delta\delta^{2}H$ values of benzene measured at the anode of the MFC (red symbol) and pseudo-anode of the control (black symbol) during continuous treatment. Values of $\Delta\delta$ were calculated by subtracting the measured isotopic value from the initial isotopic value determined at the influent.

Figure 5: Effect of flow rate on benzene and ammonium removal (A), power generation (B), and electrode potentials (C) in the MFC. B: polarization curve (solid symbol) and power density curve (open symbol); C: anode potential (solid symbol) and cathode potential (open

symbol). Different letters (a, b, c, d) placed above the bars indicate a significant difference in removal efficiencies at the different flow rates.

Figure 6: Effect of benzene and ammonium additions, and oxygen interruption on current generation in the MFC. (A): benzene injection of 15 mg/L (a1), 30 mg/L (a2), and 50 mg/L (a3); (B): NH_4^+-N injection of 20 mg N/L (b1), 50 mg N/L (b2) and 100 mg N/L (b3); (C): Interruption of O_2 supply at the cathode; (D): correlation between current generation and benzene concentration at the anode.

Figure 7: Phylogenetic distribution of 16S rRNA genes based on the order of bacteria (A) and archaea (B) detected in the MFC and control. Bacterial orders with a read abundance <1% in all of the six samples were pooled in 'others'. MFCA: MFC anode; MFCM: MFC CEM; MFCC: MFC cathode; ConA: Control pseudo-anode; ConM: Control CEM; ConC: Control pseudo-cathode.

631 Wei et al., Table 1

632

633

Parameters	Means ± Stdv
NH_4^+ (mg/L)	21.3 ± 1.6
NO_2^- (mg/L)	<0.02
NO_3^- (mg/L)	<0.1
SO_4^{2-} (mg/L)	2.4 ± 1.5
Total Fe (mg/L)	5.6 ± 0.6
Fe^{2+} (mg/L)	5.4 ± 0.8
PO_4^{3-} (mg/L)	2.3 ± 0.1
Cl^- (mg/L)	95.2 ± 5.6
Benzene (mg/L)	15.2 ± 0.6
MTBE (mg/L)	1.1 ± 0.1
COD (mg/L)	83.8 ± 2.6
BOD_5 (mg/L)	36.8 ± 4.7
TOC (mg/L)	29.0 ± 7.2
IC (mg/L)	275.3 ± 27.6
DO (mg/L)	0.05 ± 0.01
Eh (mV)	-167 ± 23
pH	7.5 ± 0.3

634 Note: Contaminated groundwater was collected during September-December 2013 from the Leuna site.

635

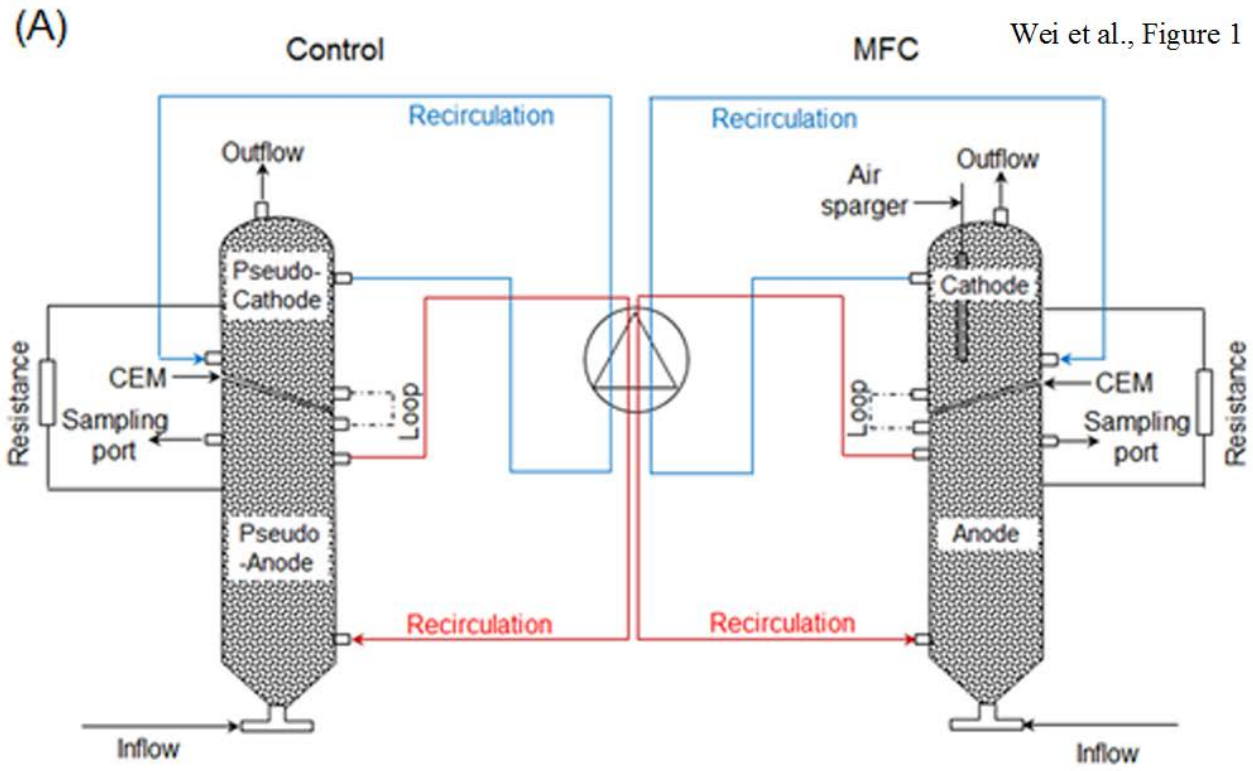

636
637
638
639
640

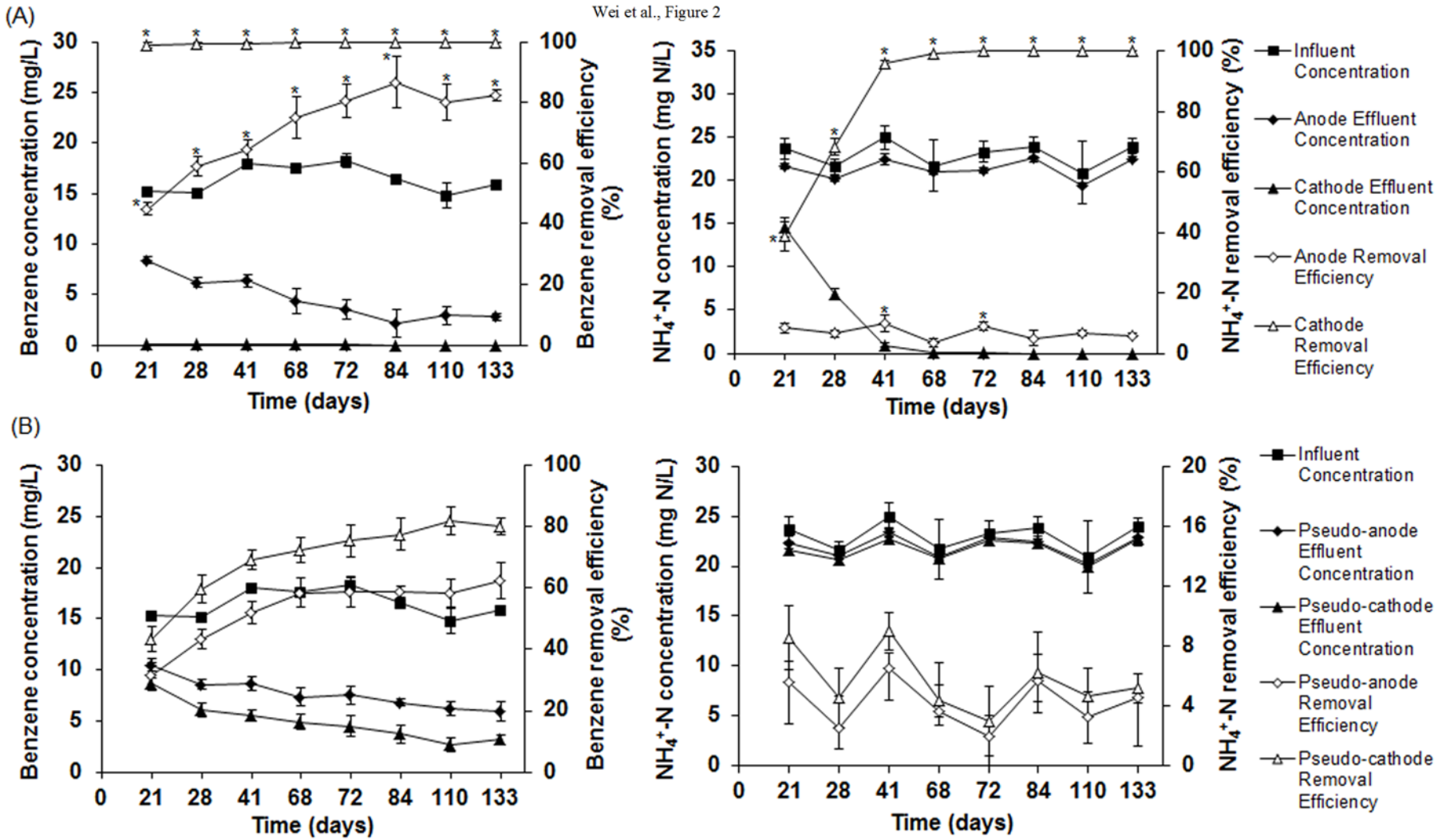

641

642

643

Wei et al., Figure 3

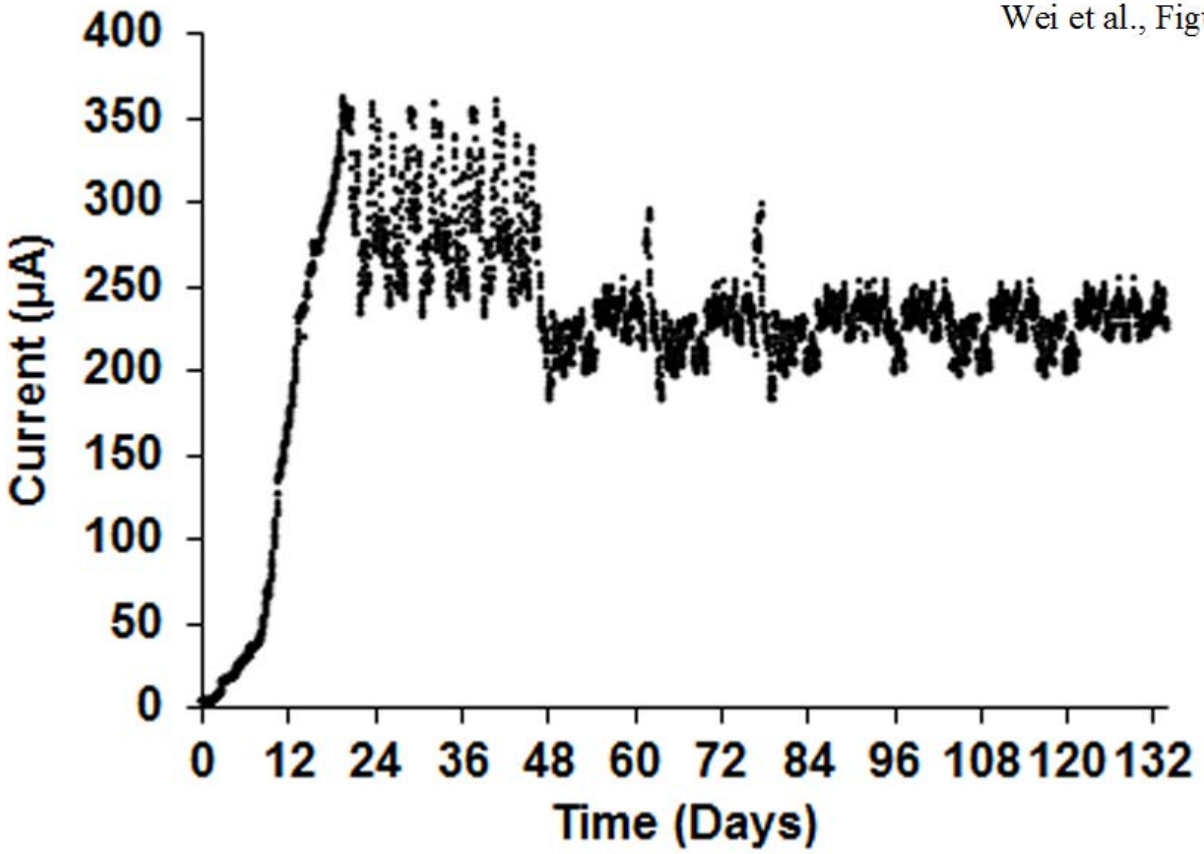

644

645

646

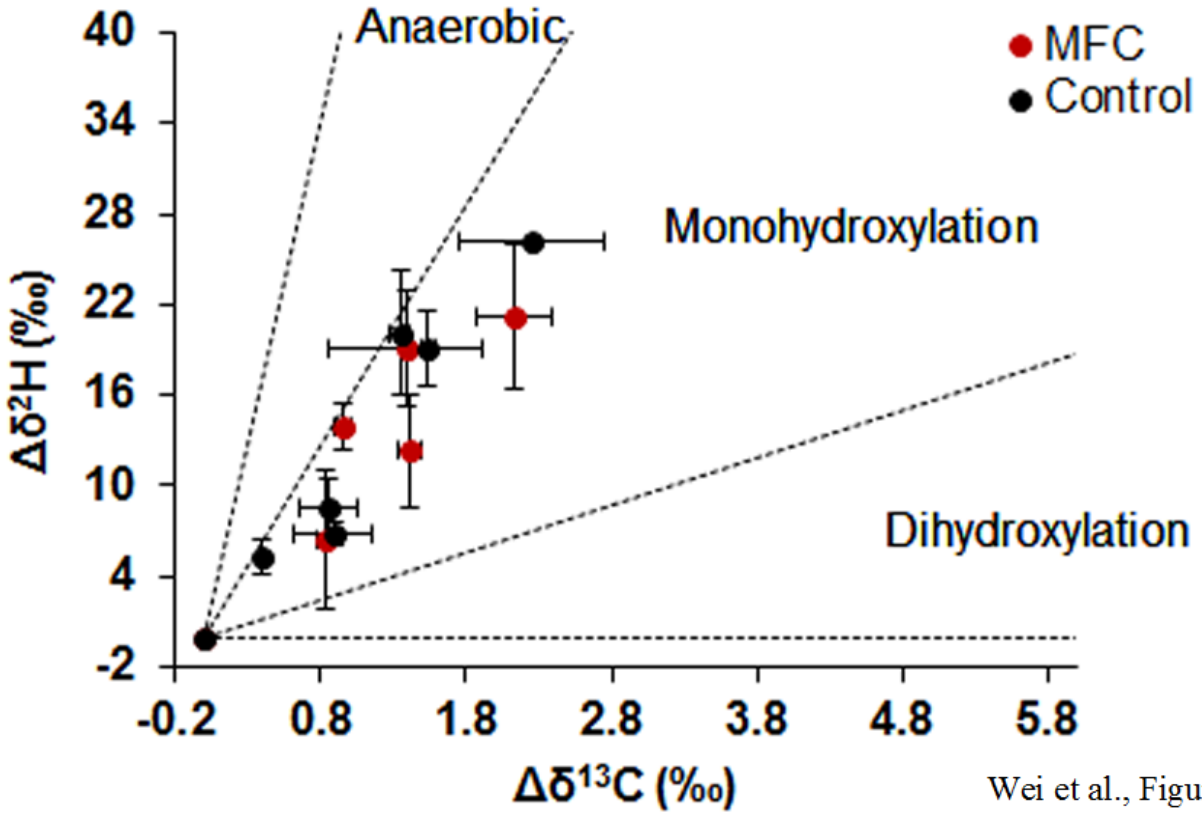

Wei et al., Figure 4

647

648

649

650

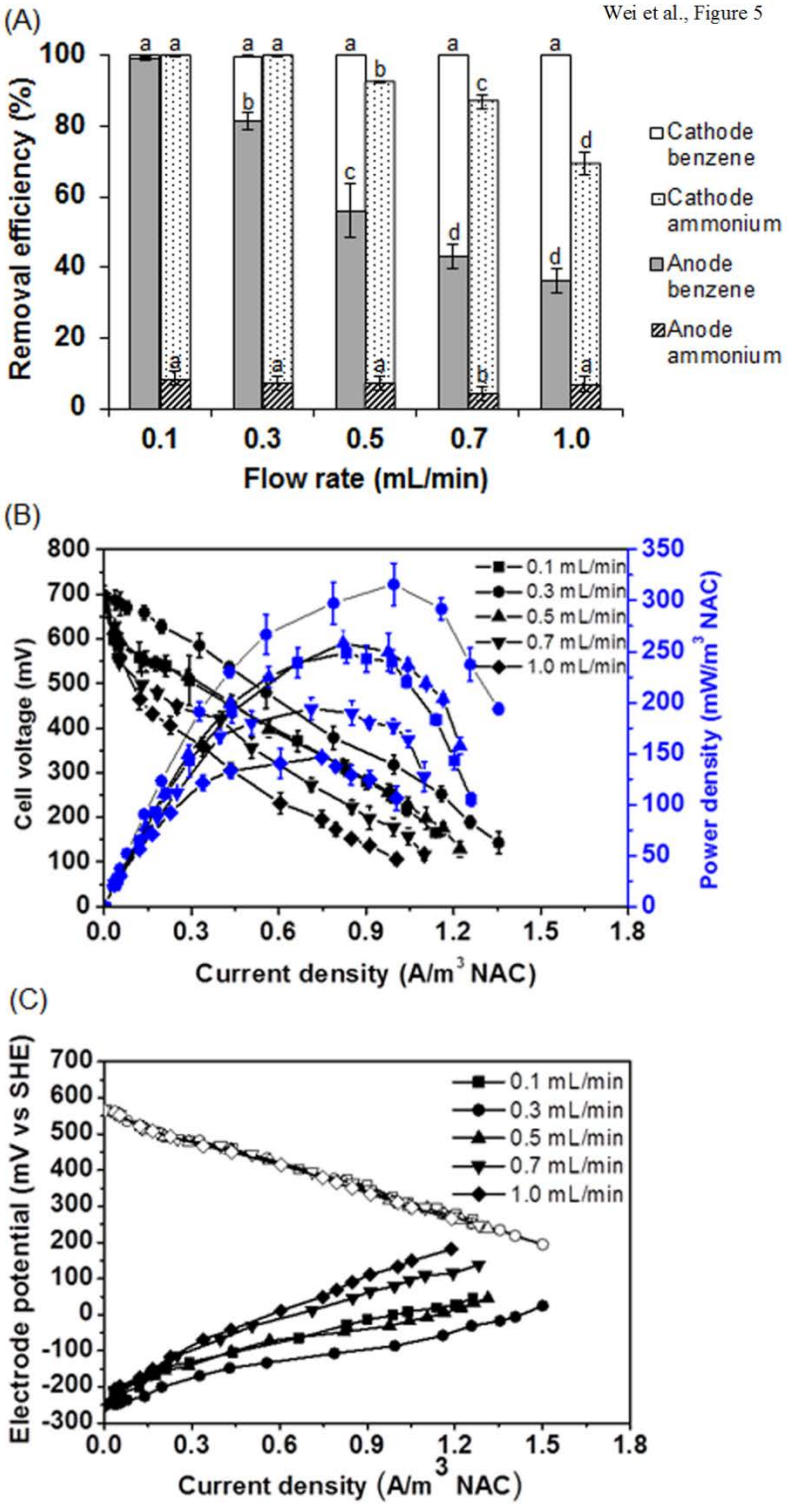

651

652

653

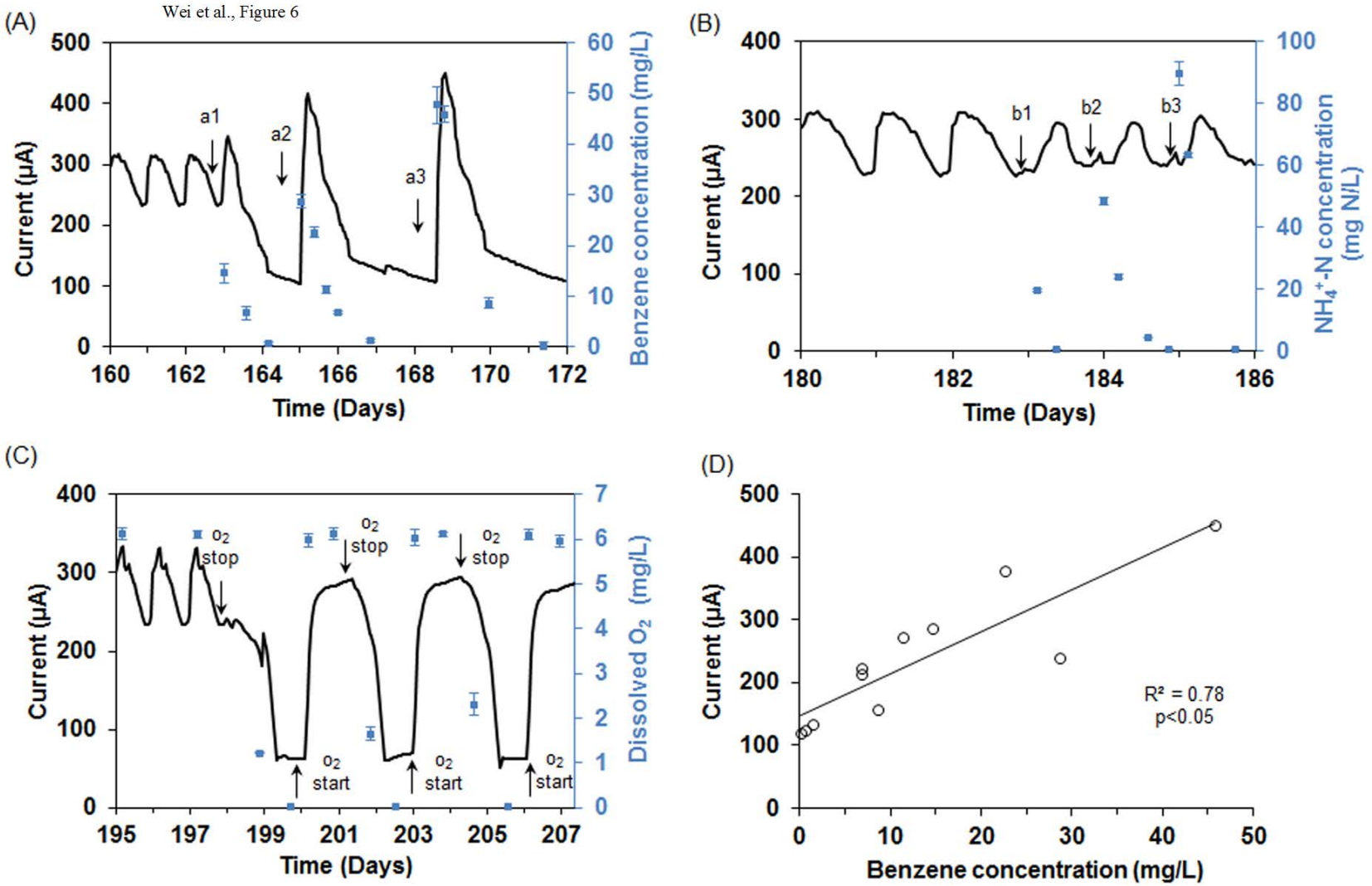

654

655

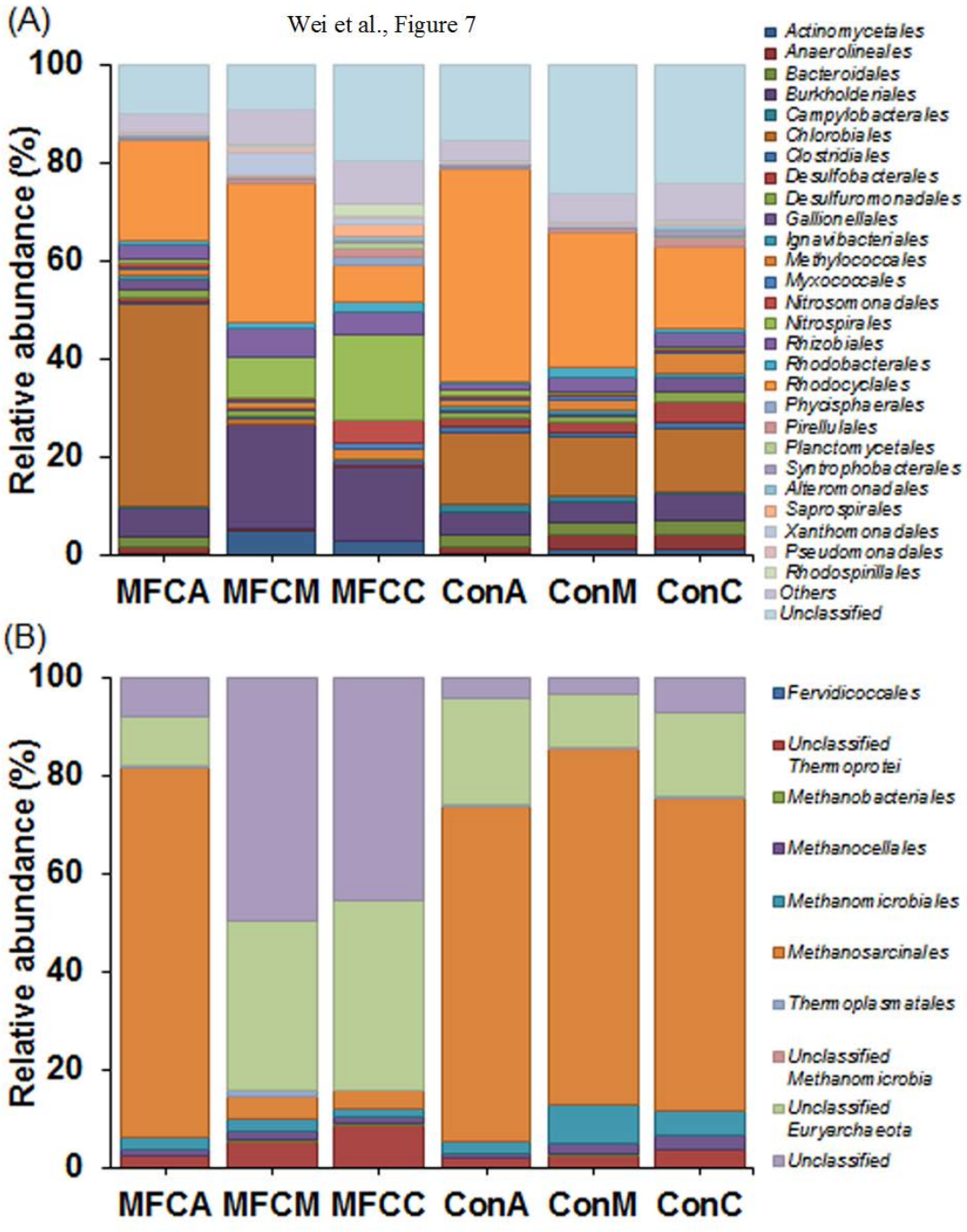

656